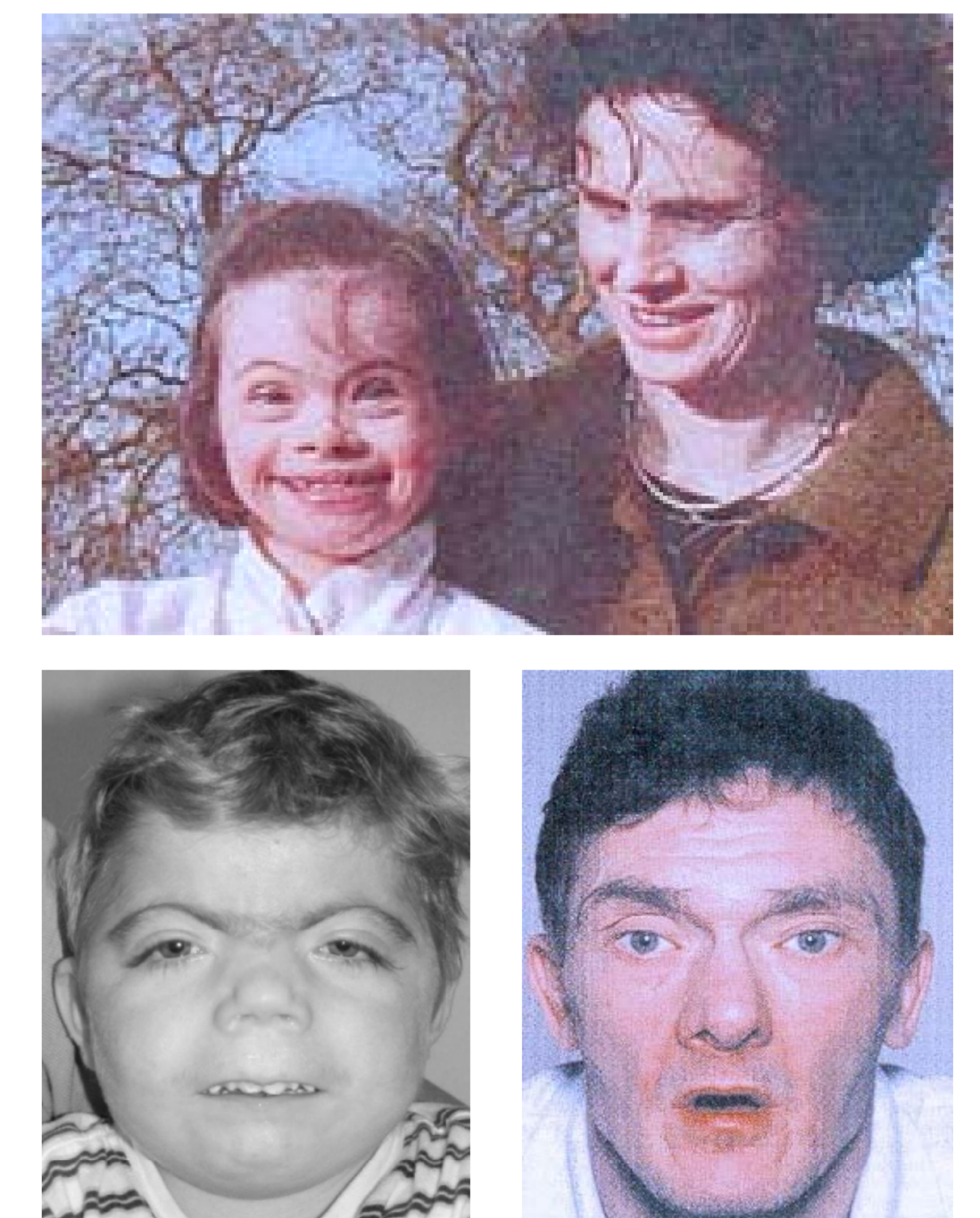


Context and summary

Craniofacial geometry has been suggested as an index of early brain dysmorphogenesis in neuropsychiatric disorders of developmental origin, like autism (1), fetal alcohol syndrome (2), schizophrenia and bipolar disorder (3). We investigate the impact of inconsistency in manual annotations when used to train automatic models for 3D facial landmark localization.

We present a new family of 3D geometry descriptors based on the asymmetry patterns present in the popular 3D Shape Contexts (3DSC)[4]. Our approach resolves the azimuth ambiguity of 3DSC, thus providing rotational invariance, at the expense of a marginal increase in computational load, outperforming previous algorithms dealing with the azimuth ambiguity.



3D Shape Contexts

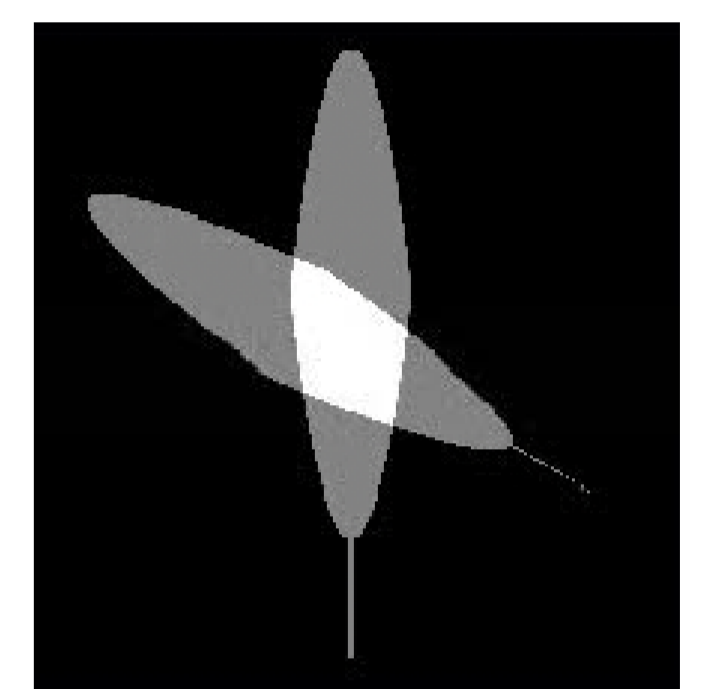
- Provide a description of local geometry based on histograms built over a spherical grid.
- Stand out due to their accuracy when used to locally search facial landmarks.
- The spherical grid is centered at the point of interest and the North pole is oriented with the normal to the surface
- Elevation and radial bins are well determined but azimuth remains ambiguous.

Asymmetry Patterns Shape Contexts

- APSC provide accuracy comparable to 3DSC but are rotationally invariant and use only half as much memory.
- APSC outperform previous rotationally invariant approaches: much more accurate than Unique Shape Contexts (USC) [5] and much faster than Harmonic Shape Contexts (HSC) [4].
- APSC can be built incrementally from a 3DSC.
 - All APSC share the same 3DSC (computed only once).
 - An APSC takes only 5% to 10% extra time to build than a 3DSC descriptor.

Asymmetry Patterns

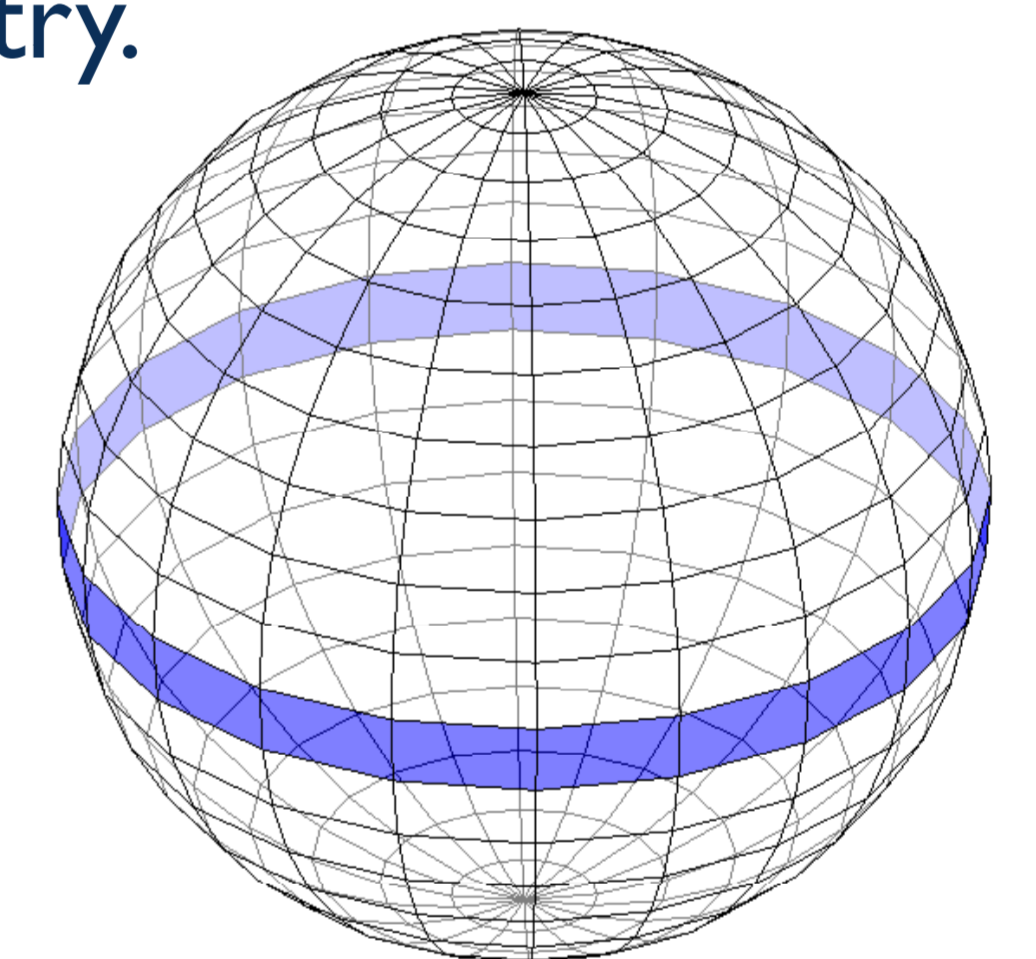
We build on a recently presented measure of approximate rotational symmetry in 2D [6], defined as the overlapping area between a shape \mathbf{m} and itself after a rotation by an angle ϕ :



$$S_c(\mathbf{m}, \phi) = \frac{\text{Area}(\mathbf{m} \cap R(\mathbf{m}, \phi))}{\text{Area}(\mathbf{m})}$$

We adapt the above to extract asymmetry patterns from a 3DSC and show that, for a sequence of bins \mathbf{m} covering all azimuth indices, the summation of absolute differences between \mathbf{m} and a rotated (shifted) version of itself is a measure of its asymmetry.

For instance, given a 3DSC descriptor \mathbf{x} we can fix the indices for elevation (i) and radius (k) and vary only azimuth (j) to obtain rings as illustrated in the figure:



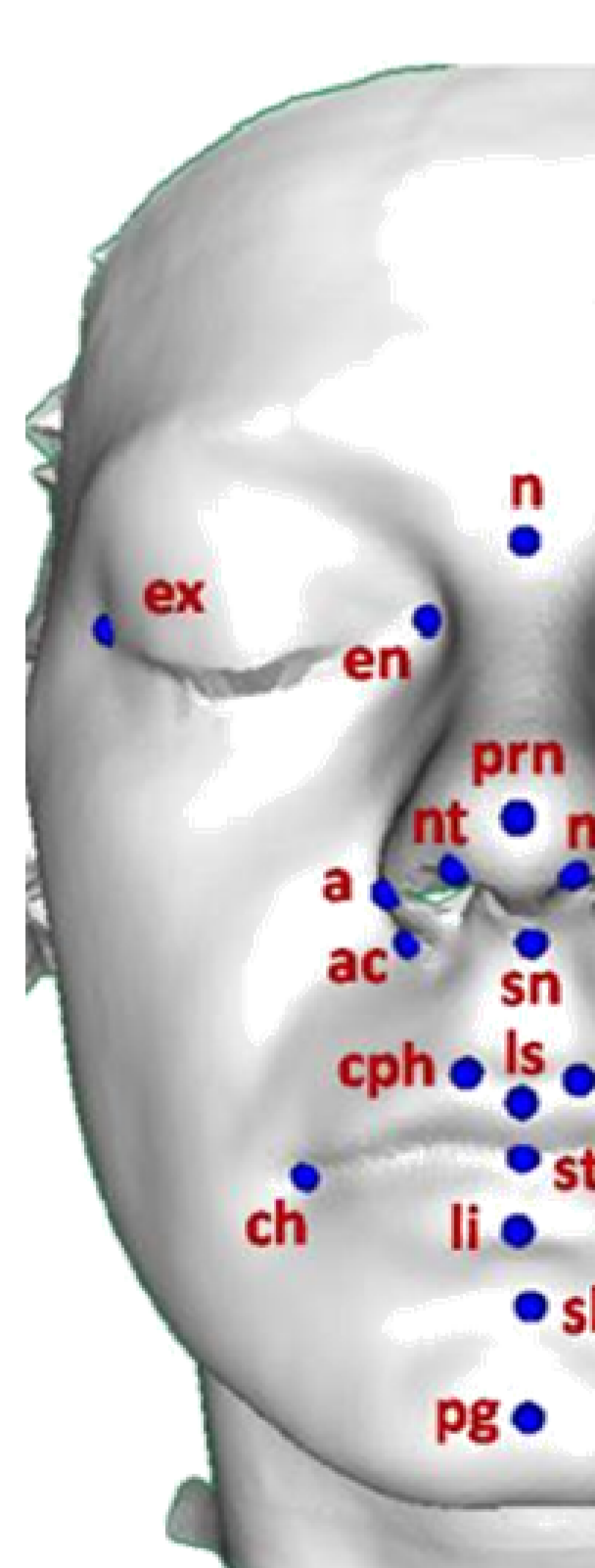
$$m_j = x_{i,j,k}$$

However, this is just a specific choice of \mathbf{m} that leads to one of many possible APSC. A few straightforward alternatives include:

- the variation of azimuth accompanied by a variation in elevation and/or radius (diagonals).
- Jointly considering two (or more) rings that are neighbors.

References

1. Ozgen HM, Hop WJ, et al. Mol. Psychiatr. 2010; 15: 300–307.
2. Mutscangwa TEM, Meintjes EM, et al. Am. J. Med. Genet. Part A, 2010; 152A:32–41.
2. Hennessy RJ, Baldwin PA, et al. Schizophr. Res. 2010; 122(1-3): 63–71.
4. Frome A, Huber D, Kolluri R, et al. ECCV, 2004, pp 224–237.
5. Tombari F, Salti S, Stefano, LD. ACM Work 3D Obj Retr 2011, pp 57-62
6. Guo, Q, Guo F, Shao J. IEEE T PAMI 32(10):1730–1743.
7. Sukno FM, Waddington JL, Whelan PF. GRAPP 2013, pp 7-17



Lmk	HSC	USC	3DSC	APSC				
				DAR	DAER	A+E	A+R	A+DAER
en (2)	1.3* (2 - 24)	1.9 (3 - 25)	1.4 (3 - 25)	1.5 (3 - 25)	1.5 (3 - 25)	1.4* (3 - 24)	1.3 (3 - 25)	1.3* (3 - 25)
ex (2)	4.5 (16 - 90)	n.p	4.3 (13 - 88)	2.9 (6 - 67)	3.9 (19 - 48)	5.4 (13 - 88)	4.7 (14 - 89)	3.1* (8 - 88)
n (2)	1.8 (3 - 200)	4.6 (5 - 12)	1.5 (3 - 200)	1.6* (4 - 200)	1.6* (4 - 64)	2.3 (4 - 200)	2.0 (3 - 200)	1.7* (4 - 200)
a (2)	1.4* (3 - 26)	n.p	1.4 (4 - 27)	2.9 (6 - 12)	n.p	2.1 (4 - 25)	1.8 (4 - 26)	2.0 (6 - 26)
ac (2)	2.1* (5 - 25)	5.8 (14 - 25)	4.7 (9 - 25)	9.0 (16 - 24)	n.p	2.3 (7 - 25)	2.1 (4 - 11)	5.1 (14 - 25)
nt (2)	2.0 (4 - 8)	12.2 (14 - 200)	8.0 (14 - 200)	6.9 (12 - 200)	7.5 (11 - 200)	2.3 (5 - 8)	2.2 (5 - 9)	6.6 (11 - 200)
prn (2)	1.4 (3 - 200)	1.4 (2 - 200)	1.2 (2 - 200)	1.3 (3 - 200)	1.3* (2 - 200)	1.3* (2 - 200)	1.3* (2 - 200)	1.3 (3 - 200)
sn (2)	1.8 (4 - 200)	n.p	1.6 (4 - 55)	1.8* (4 - 22)	2.0 (5 - 16)	1.9 (3 - 200)	1.9 (3 - 200)	1.9 (4 - 200)
ch (2)	3.8 (11 - 22)	2.4 (4 - 42)	2.1 (5 - 19)	2.5 (9 - 29)	2.9 (10 - 39)	2.8 (6 - 18)	2.9 (5 - 20)	2.3* (5 - 28)
cph (2)	2.1 (4 - 9)	13.3 (20 - 34)	8.4 (18 - 200)	7.1 (17 - 86)	7.0 (16 - 59)	n.p	7.7 (16 - 200)	2.7 (5 - 8)
li (2)	5.0 (16 - 51)	2.7 (7 - 48)	2.3 (5 - 10)	4.4 (16 - 37)	3.4 (11 - 45)	4.9 (10 - 15)	4.8 (9 - 15)	3.8 (15 - 95)
ls (2)	4.1 (6 - 14)	n.p	2.3* (8 - 46)	2.7 (8 - 13)	2.2 (6 - 11)	5.2 (14 - 200)	5.7 (10 - 54)	3.8 (7 - 200)
sto (2)	2.7* (6 - 14)	2.9 (8 - 46)	2.2 (8 - 78)	2.5* (7 - 17)	6.1 (14 - 40)	4.0 (9 - 14)	4.5 (11 - 89)	3.1 (12 - 54)
sl (2)	5.4 (10 - 54)	3.0 (10 - 18)	3.2* (11 - 27)	5.5 (13 - 79)	7.4 (16 - 29)	4.7 (11 - 77)	6.0 (12 - 84)	6.2 (17 - 62)
pg (2)	7.0 (10 - 200)	11.6 (19 - 120)	5.4 (10 - 200)	7.9 (19 - 200)	7.1 (13 - 200)	7.6 (13 - 26)	5.6* (13 - 23)	5.7* (10 - 200)

Local accuracy and neighborhood limits on 144 facial scans [7]

Abbreviation	Sequence(s) equation	Description
DAR	$m_j = x_{i,j,k+j}$	Azimuth-Radius diagonal
DAER	$m_j = x_{i+j,j,k+j}$	Azimuth-Elevation-Radius diagonal
A+E	$m_{1,j} = x_{i,j,k}, m_{2,j} = x_{i+1,j,k}$	Azimuth ring + Elevation neighbors
A+R	$m_{1,j} = x_{i,j,k}, m_{2,j} = x_{i,j,k+1}$	Azimuth ring + Radial neighbors
A+DAER	$m_{1,j} = x_{i,j,k}, m_{2,j} = x_{i+j,j,k+j}$	Azimuth ring + Azim-Elev-Rad diagonal

Examples of simple APSC descriptors

The authors would like to thank their colleagues in the Face3D Consortium (www.face3d.ac.uk), and the financial support provided from the Wellcome Trust (grant 086901/Z/08/Z) and the Marie Curie IEF programme (grant 299605, SP-MORPH).

Supported by
wellcometrust

